COMPARATIVE EXTRUDABILITY OF 6061 ALLOY AND
15 Vol % SiC PARTICULATE COMPOSITE

E.M. Herba and H.J. McQueen

Mech. Eng., Concordia University, Montreal, Canada H3G 1M8

ABSTRACT Constitutive equations were determined by torsion for 15% SiCp/6061 liquid metal mixed composite and for 6061 alloy in the ranges 10^{-2} to 5 s^{-1} and 300 - 540°. Extrusion was modeled by finite element analysis as a two dimensional slice from an axisymmetric billet, die, container, dummy block and ram. The varied conditions examined were initial billet temperature (450,475, 500°C), for extrusion ratio 31 and 2 ram speeds (2.6, 5 mm/s). With sticking friction conditions, there was a dead zone and maximum near the die corner in distributions of either velocity or strain rate (independent of material) and of either mean stress or temperature which depend on the hot strength of the materials and influence the occurrence of extrusion defects. The initial billet temperatures were calculated in order for the composite to remain with the same maximum pressures as the alloy. Comparisons are made to flow patterns determined by physical simulations and other extrusion models. The extrusion pressure ram stroke curves, which exhibit the traditional peak followed by a sharp then gradual decline due to deformation heating are compared to results of similar modeling and trial extrusions.

Keywords: *Particulate Composite, Extrusion Modeling, Constitutive Equations, Hot Deformation*

INTRODUCTION

Particulate Al matrix composites (AMC) have improved strength, creep and fatigue resistance but more importantly considerably greater modulus than the matrix alloy [1-5]. Through primary production by liquid metal mixing and secondary fabrication by traditional mechanical forming, components can be economically produced for ground transport applications [3,6]. Extrusion is capable of producing tubing for sports vehicle drive shafts with less vibration and bicycle frames with reduced flexing.

In consequence highly extrudable 6061 [7,8] both the alloy and matrix with 15% SiC reinforcements (compositions, Table 1) were subjected to torsion tests in the ranges 300-540° and 0.1 to 4 s^{-1} to determine flow stress constitutive constants and ductility [9-11]. These results were utilized in the DEFORM^{tm} finite element analysis extrusion in order to compare 6061/15% SiCp with 6061 alloy and hence to optimize the processing.

RESULTS

The stress-strain ($\sigma - \varepsilon$) curves, derived from the torsion tests described previously [9,10], are shown in Fig. 1a. The curves essentially exhibit strain hardening to a steady state plateau. At low temperature T the ductility is reduced by the decohesion at particles combined with matrix cracking enhanced by particle constraints [11]. At high T the plateaus decline gradually as a result of flow fissuring with ductilities always less than the alloy itself. The shape of the curves lends itself to the approximation of an elastic-plastic material with constant peak flow stress. The σ variation with T and $\dot{\varepsilon}$ is shown in Fig. 1b with a comparison of the experimental data with values calculated from the constitutive equation:

$$A(\sinh \alpha\sigma)^n = \dot{\varepsilon}(\exp Q/R'T) = Z$$

where material constants are A, $\alpha(\approx 0.052 \text{ MPa}^{-1})$, (R'=8.3 J/mol K), n stress exponent and Q activation energy. The Zener-Hollomon parameter embraces the two control variables $\dot{\varepsilon}$ and T. The constants for the 6061 alloy and the AMC are derived in Fig. 2 and listed in Table 1[19-20].

Examples of the detailed modeling of the extrusion are given in Fig. 3 which provides the deformation of an originally square grid in the billet and the distributions of T, $\dot{\varepsilon}$ and mean stress σ_m for extrusion of a billet 305 mm long by 178 mm diameter at a ratio R of 31 and a ram velocity V_r of 2.6 or 5 mm/s [21-24]. The extrusion die was initially at 425°C, ram at 175°C and the chamber heated to be 20 to 30°C below the billet T_b of 450 to 500°C. The physical constants taken from handbooks have been listed previously; the friction factor is taken as unity so that the metal shears internally [23]. The load stroke curves in Fig. 4 show that the peak load declines with rising T_b and declining V_r.

Essentially ram pressure P or load L rises to a maximum (P_m,L_m) until yielding occurs with material at T_b near the die exit. As plastic flow spreads in a non-uniform manner to develop the distributions illustrated, the work expended turns to heat which despite the losses to the tooling gives rise to a hot zone with the distribution in Fig. 3b. This rise in T leads to initial decline in P with stroke [7]; once the T pattern is established, the decline is due to decreased chamber friction as the billet shortens. The maximum T_m occurs at the die throat where the strain rate is also very high. The variation of T_m with the insert T_b is presented in Fig. 5a for the 6061 alloy and the 15% SiC AMC. Evidently as T_b or R rises, T_m climbs towards the incipient melting point and would give rise to an increase in surface defects. From Fig. 5b it is evident that the load decreases as both T_b and T_m rise.

The effect of V_r on T_m and maximum strain rate $\dot{\varepsilon}_m$ are shown in Fig. 6. The maximum velocity for both materials increases from about 90 to 190 mm/s for V_r of 2.6 and 5 mm s

TABLE 1 CHEMICAL COMPOSITON & CONSTITUTIVE CONSTANTS FOR 6061 & MMCS

Material	Composition wt% ***					Constitutive Constants (α=0.052 MPa^{-1})				T_{billet} (°C) for load 7x10^{6}N R=31	
	Mg	Si	Cu	Fe	Mn	Q(KJ/mol k)	A(s^{-1})	n	r ****	V_{ram}= 2.6 mm/s	V_{ram}= 5.0 mm s
6061 Al *	0.97	0.71	0.28	0.58	0.04	205	1.17x10^{12}	3.49	0.9827	450	463
10%Al$_2$O$_3$**	1.0	0.6	0.3	0.7	0.15	179.8	2.42x10^{10}	2.76	0.9879	464	488
15%SiC **	1.0	0.6	0.3	0.7	0.15	233.4	1.18x10^{14}	2.59	0.9892	479	491
20%Al$_2$O$_3$**	1.0	0.6	0.3	0.7	0.15	246	1.30x10^{15}	1.98	0.9794	489	500

*Cr 0.24, Zn 0.045, Ti 0.016, **Vol % matrix 6061, *** Remainder Al, ****r = correlation coefficient
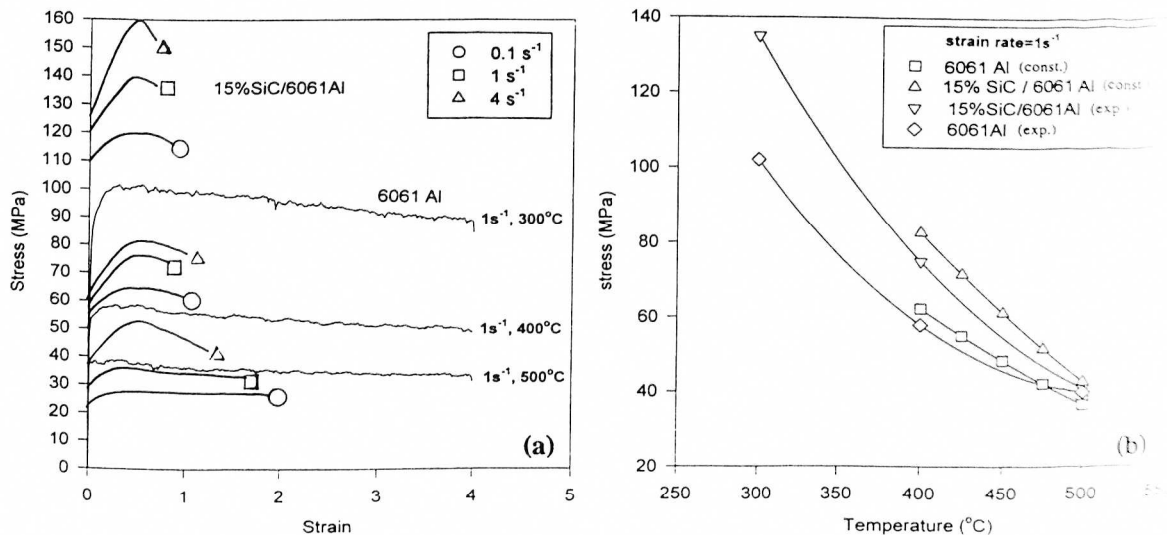

Fig 1 Hot workability of 6061 alloy and 6061/15%SiCp is presented as a) representative flow curves and b) variation of peak σ with T, the experimental being compared with that calculated from Equation 1.
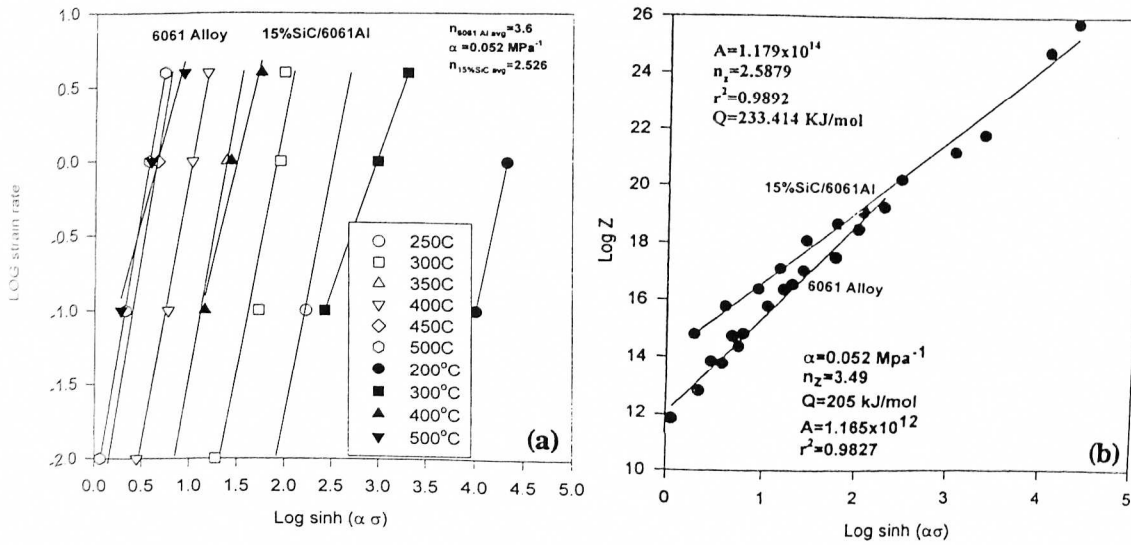
Fig. 2 Constitutive analysis according to Eq. 1 for 6061 alloy and AMC: a) log $\dot{\varepsilon}$ versus log σ and b) log Z versus sinh $\alpha\sigma$.

respectively; with doubling of ram speed there is thus a doubling of exit velocity in similarity to the rise in $\dot{\varepsilon}_m$. From Fig. 5b it is possible to determine the T_b required for the AMC to give the same L_m (7.0 N) as for 6061 at 450°C; these are presented in Table 1.

DISCUSSION

The hot workability data (Fig. 1) is a little misleading because of the much higher flow stresses of the AMC below 350°C which may become significant in the final stages of rolling or forging [6]. However between 400 and 500°C (Fig. 1b) the difference is much smaller as seen in the values calculated from the constitutive equation based on the presentation in Fig. 2 where the Z plots show r values over 0.98. The activation energy for the alloy is about 20% higher than that for aluminum; however, this is not unusual for commercial alloys due to segregated particles [25]. The composite is considerably higher but also is consistent with other AMC; those with stronger matrix alloys are usually higher [9-17].

This constitutive behavior is consistent with the microstructure which was examined by TEM. The substructures exhibit some regions (~33%) of subgrains which are smaller and less dynamically recovered (DRV) than those in the matrix alloy for the same T and $\dot{\varepsilon}$ conditions [12-19]. Other regions exhibit dense dislocation, arrays generally with very poorly developed cellularity; these tend to be close to particle clusters or in shear zones. The type of final structure (~33%) consists of discrete fine cells in the dense regions above with high misorientations indicative of dynamic recrytallization (DRX) nuclei (not usually found in the matrix alloy); DRX never spreads to any degree but does help to reduce the flow stress [16-19]. The improved ductility at high T is thus the result of the augmented DRV and DRX and possibly some degree of superplasticity [11,19,20].

The billet grid distortion and the distributions give confidence in the modeling since they are consistent with earlier simulations or model estimates [23,26,27]. The distributions emphasize that the critical region is at the die corner. The high T_m may lead to melting at segregated phases; the high $\dot{\varepsilon}$ tends to reduce the matrix resistance to cracking and to induce high stress concentrations at particle-matrix interfaces. The positive mean stress in the same regions means that there is a tensile component equaling the sum of the mean stress and flow stress. Thus there may be considerable surface damage even below the incipient melting point; particle matrix interfaces are particularly susceptible to crack initiation [6,11,18].

The formation of the hot zone before the die face is characteristic of extrusion which plays a significant role in decreasing peak extrusion load [7,8]; the decease in P or L with stroke is greater for higher peak load since there is more work and heat generation. For the 15% SiC AMC, L_m is about 160N (25%) higher than for the alloy (at R=31); L_m for the AMC can be lowered to that of 6061 by raising T_B by 30°C [23,24]. The values of T_m rise with V_r since there is more power expended and less time to dissipate the heat. Other modeling of 6061/20%Al2O3 with R=64 show that there is roughly a doubling of $\dot{\varepsilon}$ and T_m from R=31 [23,24]. It was shown that load was linearly proportional to the product of R and V_r [325] for these and two AMC with Al2O3. The load and T_m increased with rising volume fraction of particles in 6061 as illustrated in Fig. 4c [23,24]; the 15% SiC AMC lies between the 10 and 20% Al2O3 in complete consistency with intermediate strength and microstructure. It had been possible to evaluate the model for 6061/20%Al2O3 against an independent calculation and experimental extrusion of the same material; the results fit together very well [24,27]. Modeling has also been carried out on 2618 (the Concord alloy) and associated AMC with 10% or 15% Al2O3; the distributions of T,σ_m,ε and $\dot{\varepsilon}$ were similar [22]. The L_m and T_m were higher for the same conditions so that T_b had to be lowered to 425°C and V_r to 1.5 mm/s to keep T_m below the incipient melting temperature [22].
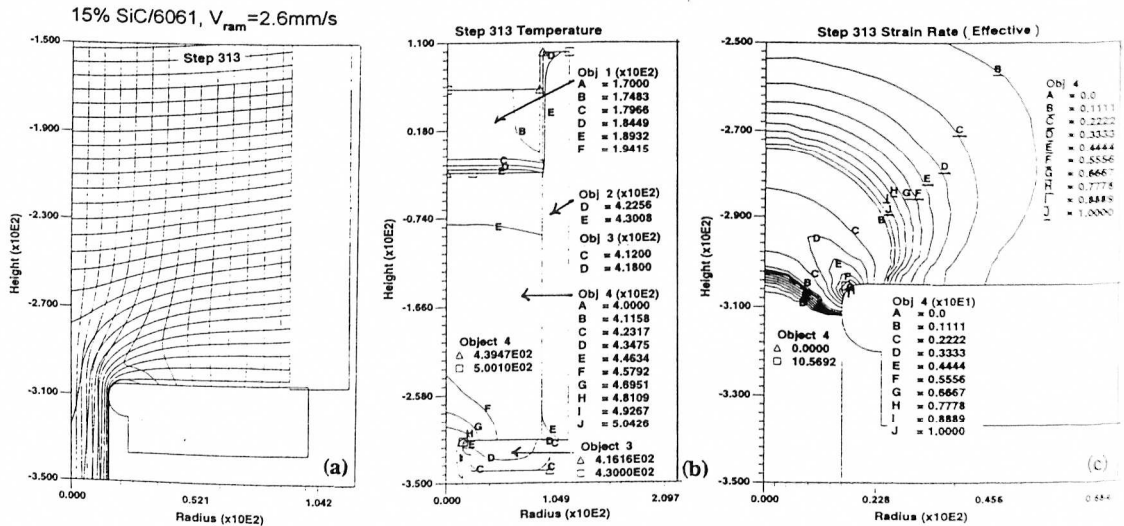

Fig. 3   Results of DEFORM t_m finite element analysis of the intense-deformation heated zone for 6061/15%SiCp (T_b = 450°C, R=31 and V_r= 2.6 mm/s): a) distortion of square grid on billet and distributions of b) T and c) $\dot{\varepsilon}$.
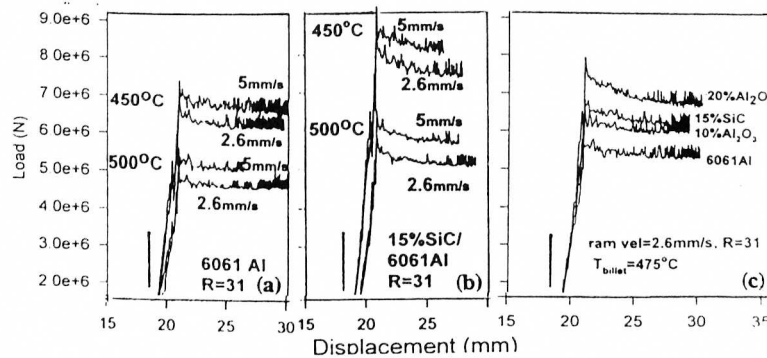

Fig. 4   Modeled effects on load-stroke curves for extrusion with R=31 of 6061 alloy and composites from variation of T_b and of V_r for a) 6061 Al b) 6061/15% SiCp and c) comparisons with 6061/10%Al2O3 and 6061/2% Al2O3 at 475°C.
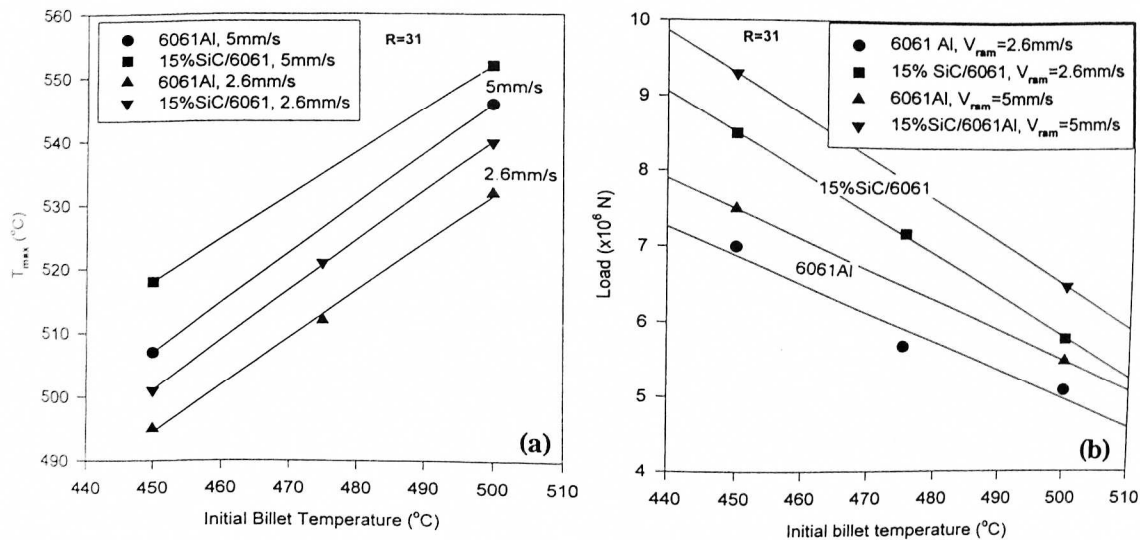
Fig. 5 Modeled influence of T_b during extrusion of 6061 and 6061/15% SiCp at R=31 on a) T_m and b) on L_m for V_r = 2.6 or 5mm/s at R=31.

CONCLUSION

The extrusion modeling with DEFORM^{tm} software provides distributions of temperature, mean stress and strain rate with maxima at the die corner, consistent with physical simulations. Under all conditions, the breakout load is higher for the 15% SiC composite than for the 6061 alloy; billet temperature would have to be raised about 30°C to make them the same. Initially the load drops rapidly with the stroke as a result of temperature rise in the deformation zone, which is greater when more work is done. The extrusion behavior of the 15%SiC AMC is intermediate between 10%Al₂O₃ and 20%Al₂O₃ composites; the latter agreed with an experimental extrusion.

REFERENCES

1   D.J. Lloyd, High Performance Composites for the 1990's, S.K. Das, C.P. Ballard and F. Marikar, eds., TMS, Warrendale, PA (1991), pp. 33-45.
2   D.J. Lloyd, Advanced Structural Materials, D.S. Wilkinson, Ed., Pergamon Press, Oxford, UK (1989), pp. 1-21.
3   F. T. Klinowicz, JOM (TMS) 48 [2] (1996) 52-57.
4   H.J. McQueen and P. Sakaris, First Canadian International Composites Conference and Exhibition, CANCOM '91, Montreal, Canada, 1991, 3C3-1 - 3C3-8.
5   H.J. McQueen and X. Xia, (Joint Canada-Japan Workshop on Composites, Kyoto, August 1996) Sci. Eng. Comp. Mat. 6 (1997) 185-200 (in press).
6   H.J. McQueen and E. Evangelista, Materials for LeanWeight Vehicles, 24-25 Nov. 1997, Gaydon, England).(In press)
7   H.J.McQueen and O.C. Celliers, Materials Forum (Australia)17 (1993) 1-13.
8   H.J.McQueen and O.C. Celliers, Can. Metal. Quart. 36.(1997) 73-86.
9   P. Sakaris and H.J. McQueen, Aluminum Alloys: Their Physical and Mechanical Properties - Proceedings ICAA3, L. Arnberg, E. Nes, O. Lohne, N. Ryum, eds., NTH-Sinteff, Trondheim, Norway, (1992), 1, pp. 554-559.
10   P. Sakaris and H.J. McQueen, Advance in Production and Fabrication of Light Metals, M.M. Avedesian et al, eds. Met. Soc., CIMM Montreal (1992), pp. 605-617.
11   H.J. McQueen, P. Sakaris and J. Bowles, Advanced Composites '93, ed. by T. Chandra, A.K. Dhingra, TMS-AIME, Warrendale, PA, (1992), pp. 1193-1198.

12   X. Xia, P. Sakaris and H.J. McQueen, Developments and Applications Of New Ceramic And Metal Alloys, R.A.L. Drew,H.Mostaghed,Eds,Met.Soc-CIMM,Montreal(1993),pp. 495-510.

13   X.Xia, P. Sakaris and H.J. McQueen, Recent Developments in Light Metals, Met. Soc. CIMM, Montreal (1994), pp. 123-134.

14   X. Xia, P. Sakaris and H.J. McQueen, Mat. Sci. Tech. ,10 (1994) 487-494.

15   X. Xia, H.J. McQueen and P. Sakaris, Scipta. Metal. Mat.,32, (1995), 1185-1190.

16   H.J. McQueen, X. Xia, E.V. Konopleva, P. Sakaris and Q. Qin, Al Alloys, Physical and Mechanical Properties, (ICAA/4, Atlanta), T. Sanders and E.A. Starke, eds., Georgia Inst. Tech., Atlanta, (1994), vol. 2, pp. 645-652.

17   H.J. McQueen, E.V. Konopleva, M. Myshlyaev and Q. Qin, Proc. Tenth International Conf. on Composite Materials, ICCM-10, (Whistler, B.C.) A. Poursartip and D. Street, eds. Woodhead Pub., Abington, (1995) vol. II, pp. 519-530.

18   H.J. McQueen, E.V. Konopleva and G. Avramovic-Cingara, Proc. 11th Intnl. Conf. Composite Materials, M.L. Scott, et al. eds., Australian Comp. Struc. Soc., Melbourne (1997) vol III, pp. 418-428.

19   H.J. McQueen and X. Xia, Recrystallization and Related Topics (Proc. 3rd Intnl. Conf., ReX '96). T.R. McNelley, (ed.), Monterey Inst. Advanced Studies, CA, 1997, pp. 603-610.

20   X. Xia, E. Herba and H.J. McQueen, Hot Workability of Steels and Light Alloys Composites, H.J. McQueen, E.V. Konopleva and N.D. Ryan (eds.), Met. Soc. CIM. Montreal (1996), pp.125-133.

21   H.J. McQueen, J. Charlton and E. Herba, Light Metals '98, Met. Soc. CIMM, Montreal 1998 (in press).

22   M. Sauerborn and H.J. McQueen, Mat. Sci. Tech, 1998 (in press)

23   E. Herba and H.J. McQueen, "Extrusion Modeling of 6061 Composites with 15% SiC and 20% Al_2O_3", Mech. Eng. Concordia Univ., Montreal, H3G 1M8

24   E.M.Herba and H.J.McQueen Mat. Sci. Tech. 1998 (in press).

25   H.J. McQueen, Hot Deformation of Aluminum Alloys, ed. T.G. Langdon and H.D. Merchant, TMS-AIME, Warrendale, PA:, (1991), pp. 31-54, 105-120.

26   H. Valberg and T. Malvik, Intnl. J. Prod. Tech 9 (1994) 428-463.

27   W.C. Chen "Extusion of Alumina Particulate Reinforced Metal Matrix Composites: Ph.D Thesis, University of British Columbia (1994) pp 65-93.
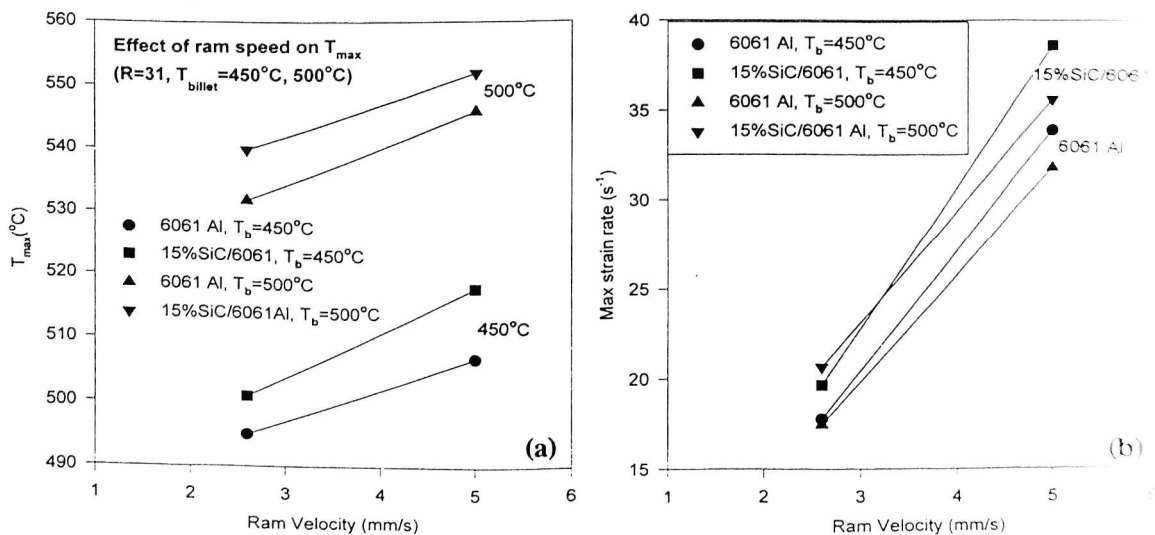
Fig. 6 Effects of ram speed in model extrusion (R=31) for 6061 Al and 6061/15% SiCp on a) T_m and b) maximum $\dot{\varepsilon}$.